Max-Planck-Institut für Meteorologie

REPORT No. 127

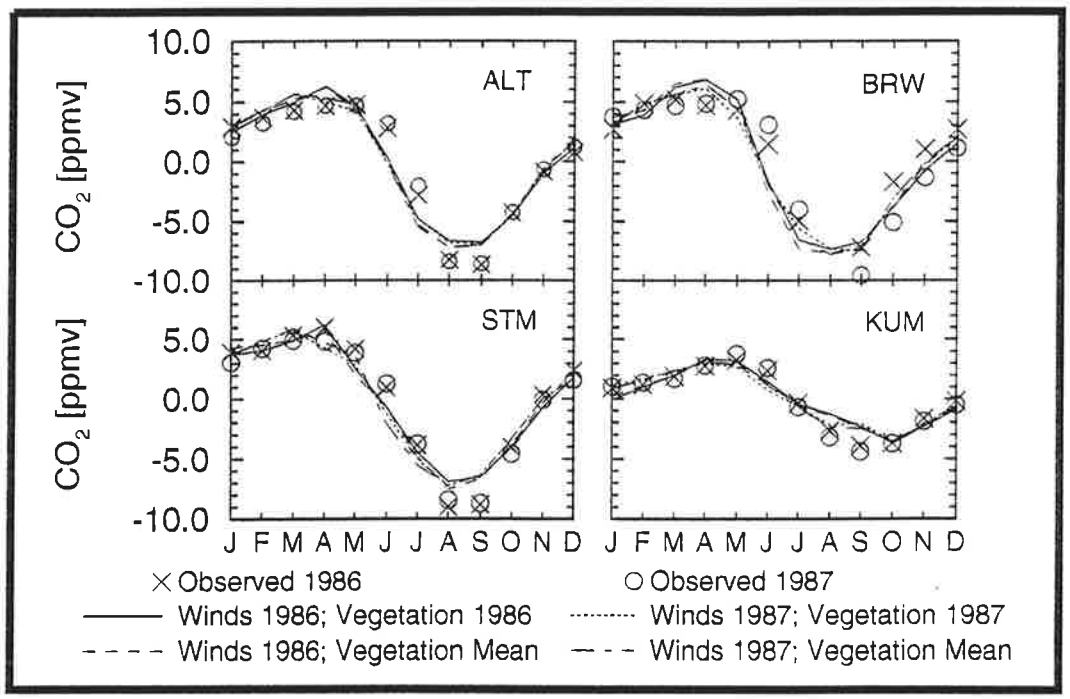

SENSITIVITY STUDY OF LAND BIOSPHERE CO_2 EXCHANGE THROUGH AN ATMOSPHERIC TRACER TRANSPORT MODEL USING SATELLITE-DERIVED VEGETATION INDEX DATA

by

WOLFGANG KNORR · MARTIN HEIMANN

HAMBURG, July 1994

ISSN 0937–1060

AUTHORS:

Wolfgang Knorr
Martin Heimann

Max-Planck-Institut
für Meteorologie

MAX-PLANCK-INSTITUT
FÜR METEOROLOGIE
BUNDESSTRASSE 55
D-20146 Hamburg
F.R. GERMANY

Tel.: +49-(0)40-4 11 73-0
Telemail: MPI.METEOROLOGY
Telefax: +49-(0)40-4 11 73-298

Revised Edition

SENSITIVITY STUDY OF LAND BIOSPHERE CO_2 EXCHANGE THROUGH AN ATMOSPHERIC TRACER TRANSPORT MODEL USING SATELLITE-DERIVED VEGETATION INDEX DATA

Wolfgang Knorr and Martin Heimann
Max-Planck-Institut für Meteorolgie
Bundesstr. 55, 20146 Hamburg, Germany

July 14, 1994

Abstract

We develop a simple, globally uniform model of CO_2 exchange between the atmosphere and the terrestrial biosphere by coupling the model with a three-dimensional atmospheric tracer transport model using observed winds, and checking results against observed concentrations of CO_2 at various monitoring sites. CO_2 fluxes are derived from observed greenness using satellite-derived Global Vegetation Index data, combined with observations of temperature, radiation, and precipitation. We explore a range of CO_2 flux formulations together with some modifications of the modelled atmospheric transport. It appears that the seasonality of net CO_2 fluxes in the tropics, which would be expected to be driven by water availability, is remarkably small, because CO_2 uptake and release are reduced simultaneously during the dry season. Consequently, tropical vegetation contributes only very little to the seaonal cycle of atmospheric CO_2, which is dominated by northern temperate and boreal vegetation, where seasonality is mostly temperature determined. We find some evidence that there is still considerable CO_2 release from soils during the northern-hemisphere winter. An exponential air temperature dependence of soil release with a Q_{10} of 1.5 is found to be most appropriate, with no cutoff at low freezing temperatures. This result is independent of the year from which observed winds were taken. This is remarkable insofar as year-to-year changes in modelled CO_2 concentrations caused by changes in the wind data clearly outweigh those caused by year-to-year variability in the climate and vegetation index data.

1 Introduction

During recent years there has been a growing perception of the role the terrestrial biosphere plays in global carbon cycling. An increasing need is felt to understand seasonal as well as interannual changes in biospheric carbon cycling, and in particular how they are related to climate fluctuations. One approach to modelling these processes is to start at the plant physiological level and eventually extend the model to the global scale (Running 1992). Such global models can then be tested by coupling model-predicted CO_2 fluxes to an atmospheric tracer transport model and comparing the seasonal cycle of simulated and observed CO_2 concentrations at various monitoring sites, because plant activity introduces by far the largest seasonal variation found in atmospheric CO_2 concentrations (Keeling et al. 1989).

In this study we explore in how far atmospheric CO_2 records can provide a constraint on global vegetation modelling. Instead of applying a detailed model with a multidude of parameters, though presumably more accurate, we choose a number of simple, globally uniform formulations of biosphere-atmosphere CO_2 exchange that reflect basic physiological concepts, thereby reducing the number of parameters to a minimum. We test modifications in input data and a variety of model formulations and parameter settings against the observed seasonal cycle of atmospheric CO_2 concentration. The results of this study can also serve as an independent test for global mechanistic ecosystem models (e.g. Melillo et al. 1993, Janacek et al. 1991, Running and Hunt 1993, Raich et al. 1991).

2 Basic concepts

As explained above, we seek a formulation of biosphere-atmosphere CO_2 exchange based on observational data that with maximum simplicity is still able to accommodate fundamental ecophysiological concepts. Consequently, we reduce the number of carbon fluxes to two, i.e. to Net Primary Productivity (NPP) and Soil Release (SR). For the moment, we consider NPP to be that part of photosynthesised carbon that remains in living plant matter and is not lost through autotroph maintenance or growth respiration. This definition will be reconsidered in Section 6.2. We further assume that all vegetation is in a steady state, so that there is no net gain of biomass after one year and the net ecosystem production equals zero. Therefore, NPP is exactly balanced by SR, under which we subsume all heterotroph respiration from soils and plant litter. In order to reduce the number of parameters to a minimum, we seek a globally uniform formulation of both fluxes and do not introduce any biospheric carbon pools.

As input data we use climate observations, and the satellite-derived Normalized Difference Vegetation Index (NDVI) to monitor photosynthetic activity of vegetation. It has been demonstrated that the NDVI, defined as the difference of the reflectivities in the near-infrared minus red divided by their sum, is a reasonable measure of light interception of vegetation formations, und thus an indicator of photosynthetic rate per incidident radiation under non-stress conditions (Kumar and Monteith 1981, Tucker

and Sellers 1986, Myneni et al. 1992, Asrar et al. 1992).

We choose a spatial resolution of 0.5^o, thus reflecting the high variability found in vegetation formations, and a time step of one month for the calculation of NPP and SR. Biospheric CO_2 fluxes are fed into a three-dimensional atmospheric tracer transport model, TM2, a modified version of the one developed by Heimann and Keeling (1989) with 7.83 by 10.00 degrees spatial resolution and 9 layers in the vertical (Heimann 1994). Eventually, we compare the observed seasonal cycle at various monitoring stations to the simulated seasonal cycle in the corresponding grid boxes of the TM2.

3 Data

As observed climate data we take monthly means of precipitation, surface temperature, shortwave, and thermal radiation from short-range weather forecasts by the European Centre for Medium-Range Weather Forecasts (ECMWF) from May 1985 to April 1989. The four-year period lies between two major changes of the forecast model (Arpe, 1991). We use the mean annual course of NDVI data from the same period as given by the Global Vegetation Index data set based on measurements on board NOAA-9 and NOAA-11 satellites with the Advanced Very High Resolution Radiometer (Gallo 1992). The data set accounts for the different pre-flight calibrations of the two satellites, however, we do not correct for temporal evolution of calibration. Monthly composites are formed by taking the highest NDVI value within each month in order to minimize the effect of cloud contamination. The data are then brought to a common spatial resolution of 0.5 degrees, by averaging the original Mercator projected NDVI data with 10.4 minutes resolution at the equator, and the ECMWF data by selecting the nearest 1.125 degree grid cell of the forecast model. A more appropriate method would have been to average the single channels before forming the NDVI. However, the data set used does not contain such information, and the difference between the two calculations should be small and insignificant for a global sensitivity study.

The TM2 is run with observed winds of both 1986 and 1987 from ECMWF analyses, which gives an indication of the uncertainties induced by changes in atmospheric transport patterns. Observed CO_2 concentrations were taken from the NOAA Climate Monitoring and Diagnostic Laboratory's flask sampling program (Conway and Tans 1990, CDIAC 1991). The mean seasonal cycle and the variance of the monthly values are computed from data records of 1980 to 1990, as far as they are available, by subtracting the long-term trend, which itself is fitted to the annual means of the data records using Hermite cubics.

4 Model development and simulations

4.1 Strategy

In this study we execute the following main steps: *First*, we simulate the seasonal cycle of land biosphere CO_2 fluxes with the mean annual course of the ECMWF climate data and the NDVI. *Second*, the fluxes are fed to the TM2, which is run over four years with the same annual course of CO_2 fluxes until a steady state is reached. *Third*, we write out the seasonal cycle during the last year of the simulation from the TM2 boxes corresponding to various monitoring sites (cf. Table 1), and compare this to the observed mean seasonal cycle (cf. Section 3). The aim is to test the sensitivity of the model against modifications in input data and varying formulations of NPP and SR. In order to assess the effect of year-to-year changes of vegetation activity, we also perform simulations based on climate and NDVI data from only 1986 and 1987, respectively, thereby running the TM2 with the wind data from the same year.

A significant problem in assessing how well the model reproduces global biosphere-atmosphere CO_2 exchange lies in the uncertainties concerning non-biospheric seasonal CO_2 fluxes. For the northern hemisphere, as a result of the large land masses and the effective barrier provided by the intertropical convergence zone, the situation is much more favourable than for the southern hemisphere, because the seasonal cycle is far more pronounced, and almost entirely of biospheric origin (Heimann et al. 1989, Nakazawa et al. 1993). In contrast, for tropical and southern-hemisphere stations the seasonal cycle is about equally influenced by biospheric and non-biospheric effects, which are mainly oceanic CO_2 exchange and, at tropical stations, CO_2 from fossil fuel burning that is advected seasonally by the monsoon circulation. An additional contribution could come from biomass burning, not captured in our model. There is still too little known about the seasonality of oceanic CO_2 fluxes to attempt incorporating them into this study. Therefore, we devise two different test criteria for the two hemispheres.

One test criterion is provided by a cost function, J, using observations from a number stations at northern latitudes:

$$J = \frac{1}{n} \sum_{i=1}^{n} \frac{c_{i,obs}^2 - c_{i,sim}^2}{s_{i,obs}^2} \qquad (1)$$

i runs over 12 months times 5 stations as listed in Table 2, $c_{i,obs}$ and $c_{i,sim}$ are observed and simulated CO_2 concentration of the mean seasonal cycle with the convention that the sum over one year equals zero. $s_{i,obs}^2$ is the variance of the mean seasonal cycle of a particular station and month. In Equation 1 we do not account for correlations between different stations. Instead, we have tried to choose a set of stations that is spread out fairly evenly across the northern hemisphere to avoid groups of highly correlated stations, since this would introduce a bias towards regions with high coverage.

For the southern hemisphere, we only take the difference in amplitude between the modelled and observed seasonal cycle as a test criterion. In the simulations by Heimann et al. (1989) it was shown for stations south of the equator that the

Table 1: Monitoring stations used for computing the cost function, J, from north to south.

Station	Code	Latitude	Longitude	Height [m]	Period
Point Barrow	BRW	71.3°N	156.6°W	11	1980-1990
Ocean Station "M"	STM	66.0°N	2.0°E	6	1982-1990
Cold Bay	CBA	55.2°N	162.7°W	11	1980-1990
Terceira Island, Azores	AZR	38.8°N	27.1°E	30	1980-1990
Cape Kumukahi, Hawaii	KUM	19.5°N	154.8°W	3	1980-1990

biospheric signal alone has about the same amplitude as the total signal comprising biospheric, oceanic and anthropogenic CO_2 sources. We further assume that biomass burning, not included into the study by Heimann et al., will not significantly affect the amplitude of the observed signal. We can therefore assume that if a simulated biospheric seasonal cycle has an amplitude considerably larger than observed, the difference could not be made up by fluxes from other sources.

4.2 Carbon uptake

When developing a formulation for NPP we follow Monteith (1977) who suggested a model for crops that relates annual NPP to the sum of absorbed Photosynthetically Active Radiation (PAR). Furthermore, it has been noted that several vegetation indices calculated from reflectances of red and near-infrared radiation, including the NDVI, are approximately linearly related to the percentage of PAR intercepted by the plant canopy (Kumar and Monteith 1981, Asrar et al. 1984, Myneni et al. 1992). Asrar et al. (1992) also showed for the NDVI that this still holds for strongly heterogeneous vegetation distributions, such as desert shrubland. The two assumptions were combined by Goward et al. (1985) who found a good linear relationship between the annual sum of NDVI and annual NPP for a variety of North American biomes. Additionally, Tucker and Sellers (1986) developed a leaf physiological model that again showed a reasonably linear relationship between the Simple Ratio Vegetation Index and photosynthetic rate per unit of PAR. All these models suggest a functional form for NPP that is proportional to NDVI times PAR, which is itself a constant proportion of incoming shortwave radiation. However, they assume that the vegetation is not water, nutrient or temperature limited.

We believe that nutrient limitation as a long-term effect will largely be reflected by a low NDVI, so that it does not have to be accounted for explicitly. As to temperature limitation, we find that setting NPP to zero whenever monthly means of temperature fall below 0°C has only a small effect, despite the large areas of boreal and temperate evergreen forest. This is partly a result of low PAR during winter in those areas, and partly an artifact of the data processing procedure for the NDVI, dropping all values whenever solar elevation is low (Gallo 1992), which coincides reasonably well with freezing temperatures during winter. We decide to ignore any temperature dependence of NPP, and expect the most significant effect to come from

water limitation.

This effect is illustrated in a study by Running and Nemani (1988), who used a regional, process-oriented forest model (Forest-BGC) to calculate photosynthesis of various forest sites, and compared this to NDVI measurements. They found that though both follow closely throughout the year when the model is run for sites with sufficient water availability, photosynthesis can almost cease while NDVI stays high in forests under substantial water stress. This demonstrates an important ability of trees: to control their water balance actively, without withering. In contrast, grasslands were found to react to sinking moisture availability by falling NDVI (Gao et al. 1992). This different behaviour of grass- and tree-like vegetation has important consequences for modelling seasonal NPP based on NDVI globally.

We do not consider differentiating between the two vegetation types, e.g. using an existing vegetation map, in order to keep to our initial concept of global uniformity of the model. Instead we consider two alternative formulations:

$$\text{NPP} = A * \text{NDVI} * \text{AET/PET} * R_S \quad (2a)$$

$$\text{NPP} = A * \text{NDVI} * R_S \quad (2b)$$

In Equation 2a we take as a measure of water stress the ratio of actual evapotranspiration (AET) divided by potential evapotranspiration (PET) calculated with a bucket model developed by Prentice et al. (1993). The bucket model uses monthly means of incoming solar and thermal radiation and precipitation, which are interpolated linearly to daily values, and has a constant field capacity of 150 mm. R_S stands for solar radiation, and A is a globally uniform efficiency constant that has to be fitted to the observed seasonal cycle of CO_2. (A is not the same for both formulations.)

4.3 Carbon release

In formulating SR, we follow Bonan (1991) and Norman et al. (1992) who both used, apart from minor additional factors, soil moisture times an exponential function of soil temperature. The study by Norman et al. was over a grassland site, whereas Bonan's was on Alaskan boreal forests. Bonan assumes that his exponentiall temperature dependence is also valid during winter, with no cutoff at low temperatures to account for freezing conditions. His assumption was based on previous measurements (Vogt et al. 1980, Moore 1983, Stohlgren 1988, Taylor and Jones 1990). In our study, we use surface air temperature instead of soil temperature, and soil moisture is replaced by AET/PET, which follows soil moisture closely in the one-layer bucket model used. This seems reasonable, since annual AET was found to be correlated with litter decomposition (Meentemeyer 1978).

However, the processes governing soil release are immensely complicated, and it is not clear how water availability relates quantitatively to microbial activity. Therefore we also consider a formulation without a water stress factor. Furthermore, other studies (e.g. Heimann and Keeling 1989) have assumed that when the temperature falls below a certain threshold the soil can be regarded as completely frozen, bringing soil respiration to a halt. We combine these different assumptions, and obtain four

Table 2: Results of the simulations to test the various formulations of NPP and SR and a range of values for Q_{10} . In each line we give the value of the cost function J after optimizing global photosynthetic efficiency, A, which is given in units of gC per MJ of PAR. The value for global annual NPP (glNPP) is also displayed in GtC. Bold numbers indicate an optimal value for Q_{10}. The error in A resulting from uncertainties in the observed CO_2 concentration is generally around 1.1%.

Formulation	NPP Equ.	SR Equ.	Q_{10}	winds	J	A	glNPP
I	2a	3a	1.2	1987	3.94	0.39	45
	AET/PET	AET/PET	**1.5**		**3.00**	**0.55**	**63**
			1.9		5.89	0.79	91
			2.4		21.14	0.94	108
			1.2	1986	4.36	0.39	44
			1.5		**3.39**	**0.54**	**62**
			1.9		5.86	0.79	91
II	2a	3b	1.0	1987	2.67	0.53	61
	AET/PET	AET/PET	1.1		2.87	0.58	67
		cutoff	1.2		3.32	0.64	73
			1.5		6.69	0.81	93
			1.9		17.91	0.94	108
III	2a	3c	1.0	1987	4.91	0.32	37
	AET/PET		1.2		3.44	0.42	47
			1.5		**2.88**	**0.59**	**68**
			1.9		8.15	0.83	96
IV	2a	3d			not used		
	AET/PET	cutoff					
V	2b	3a	1.2	1987	4.92	0.32	47
		AET/PET	**1.5**		**3.58**	**0.45**	**66**
			1.9		4.79	0.66	96
VI	2b	3b	1.0	1987	2.71	0.42	62
		AET/PET	1.2		2.67	0.52	76
		cutoff	1.5		4.25	0.67	98
			1.9		11.85	0.84	123
VII	2b	3c	1.2	1987	3.79	0.37	54
			1.5		**2.76**	**0.53**	**78**
			1.9		8.06	0.76	112
			1.2	1986	4.17	0.36	53
			1.5		**3.14**	**0.52**	**77**
			1.9		7.92	0.76	112
VIII	2b	3d	1.0	1987	2.40	0.48	70
		cutoff	1.2		2.91	0.59	87
			1.5		7.55	0.76	112
			1.9		23.76	0.80	118

alternative formulations:

$$\text{SR} = B * Q_{10}^{T/10} * \text{AET/PET} \tag{3a}$$

$$\text{SR} = \begin{cases} B * Q_{10}^{T/10} * \text{AET/PET} & \text{for} \quad T \geq -10^{o}C \\ 0 & \text{for} \quad T < -10^{o}C \end{cases} \tag{3b}$$

$$\text{SR} = B * Q_{10}^{T/10} \tag{3c}$$

$$\text{SR} = \begin{cases} B * Q_{10}^{T/10} & \text{for} \quad T \geq -10^{o}C \\ 0 & \text{for} \quad T < -10^{o}C \end{cases} \tag{3d}$$

T is the surface temperature, Q_{10} an empirical constant, and B is determined by the condition that SR and NPP balance over one year in each grid cell. (Unlike A, B is not globally constant.) Values for Q_{10} found in the literature vary between 1.3 and 3.3 (Raich and Schlesinger 1992), Bonan (1991) uses 1.91 for boreal forests, and Norman et al. (1992) 1.44 for a grassland site under warm conditions. These values are, however, related to soil temperature. In this study, we leave the size of Q_{10} open and take it as another fitting parameter.

4.4 Simulations

We run a variety of simulations with differing combinations of the Equations 2 and 3 for NPP and SR, with values for Q_{10} varying between 1.0 and 2.4, as displayed in Table 2. With B determined by the condition of local flux balance over one year, the remaining undetermined parameter is the global photosynthetic efficiency, A. Since tracer transport can be assumed linear, A only serves as a scaling factor for the simulated concentrations $c_{i,sim}$ in Equation 1. Therefore, we fit A after each run analytically by minimizing J at a fixed value of Q_{10}. The optimum of each formulation can then be estimated by taking the Q_{10} that achieves the lowest value of J, and the corresponding optimal value of A.

5 Results

5.1 Major tests

We show the results of various seasonal-cycle simulations in Table 2 and Figure 1. Table 2 shows the results gained from applying the first test criterion of Section 4.1, indicating the NPP and SR formulation chosen, Q_{10}, the optimized value of the cost function J, the corresponding value of A, and the global annual NPP (glNPP). Not that the ratio of A to glNPP is constant for a given formulation of NPP. The error in A at fixed Q_{10} that results from the uncertainty, $s_{i,obs}$, in the observed values, $c_{i,obs}$, is about 1.1% for all cases.

Figure 1 shows the observed and simulated seasonal cycle for all formulations not using a low-temperature cutoff for two southern-hemisphere stations. (This cutoff has virtually no effect at these stations.) The first station, Cape Grim, Tasmania (CGO, 41°S, 145°E), represents the CO_2 signal in the southern temperate zone, whereas the

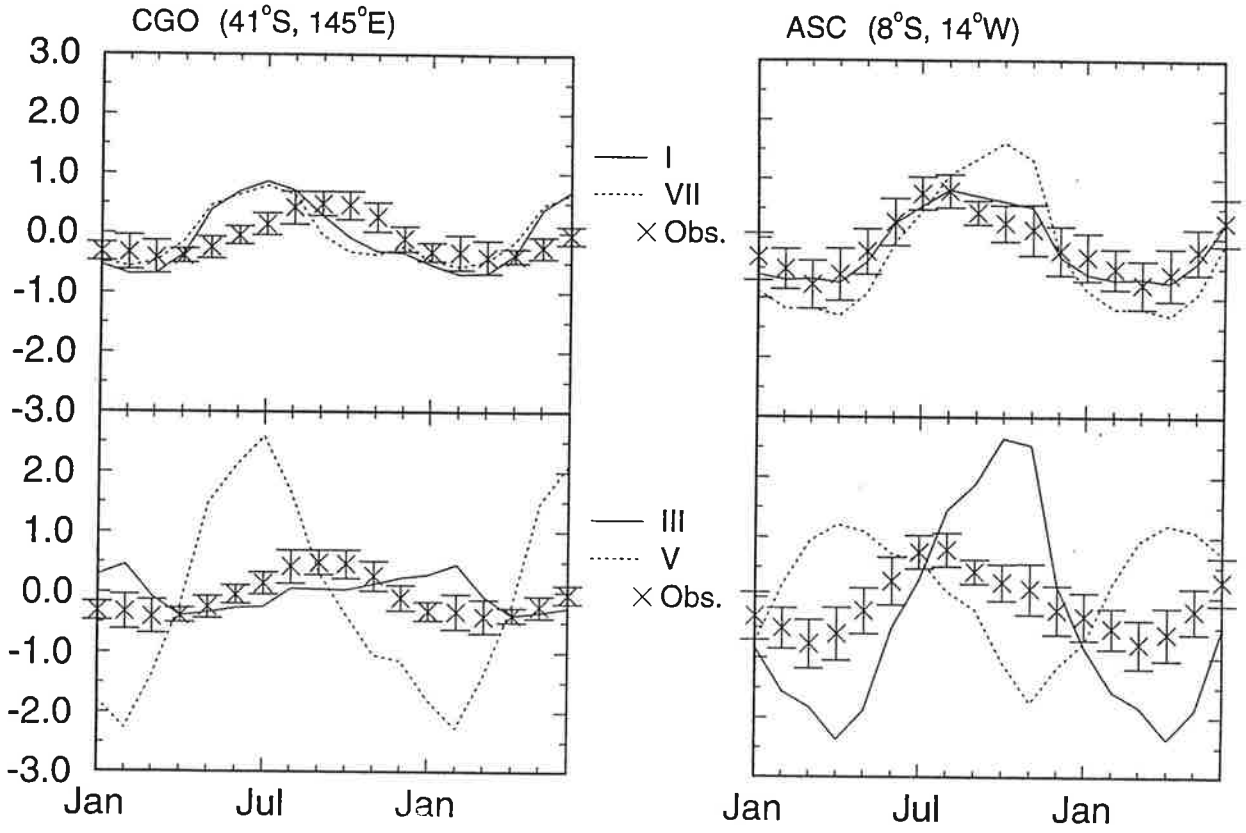

Figure 1: Simulated and observed seasonal cycle at two southern-hemisphere stations, Cape Grim (CGO, 41°S, 145°E) and Ascension Island (ASC, 8 °S, 14 °W) for all formulations not using a low-temperature cutoff. Error bars for observed values indicate $s_{i,obs}$. Simulations cannot be expected to match observations exactly because of the additional seasonality resulting from other CO_2 sources, mainly oceanic. Although the seasonal behaviour of oceanic sources is still disputed, we know that adding the resulting oceanic signal to the simulated biospheric signal would not markedly change the simulated amplitude.

second station, Ascension Island (ASC, 8°S, 14°W), is ideally situated to receive the CO_2 signal from the tropical and subtropical vegetation of southern Africa.

Comparing the amplitudes of the observed and simulated signals in Figure 1, we find that both Formulation III and V clearly fail the second test criterion. It is interesting that III does not fail at CGO, but all the more clearly at ASC, whereas V fails at both stations. At ASC, this behaviour demonstrates the opposite seasonality of tropical drought-seasonal vegetation in the two formulations, as we will see in Section 6.3. For comparison, in the model of Heimann et al. (1989), oceanic fluxes account for a signal of around 1 ppmv amplitude, and industrial CO_2 for less than 0.3 ppmv at Baring Head, New Zealand, at 41°S, 175°E, which is the nearest station to CGO used in that study. This makes it clear that even without further knowledge about the seasonality of oceanic CO_2 fluxes, we can evidently reject Formulations III and V, and with them IV (not used) and VI, since the low-temperature cutoff has almost no effect in the latitudes concerned.

Looking at the results in Table 2, and considering that most estimates of glNPP lie between 50 and 60 GtC (see Section 6.2), it appears that whenever Q_{10} is larger than 1.5, the value for glNPP after optimizing A comes out rather high and at the same time the cost function deteriorates in all simulations. With Formulations I, III, V and VII, all using no cutoff, we find a clear optimum with a Q_{10} close to 1.5 and NPP in the range that was expected, or slightly higher. This picture does not change when going from 1987 to 1986 wind data, although fits appear to be generally somewhat inferior. In contrast, values for Q_{10} cited in the literature are typically higher than 1.5. We attribute this to the fact that we derive our fluxes from air temperature, not from soil temperature. Among these four cases, we find that Formulations V and VII achieve the best fits, whereas Formulations I, III and V have a glNPP somewhat closer to commonly assumed values. It is interesting to note that very close values for A are found in both I and VII, whereas glNPP is significantly higher in VII. This illustrates that the simultanious reduction of NPP and SR through the drought-stress factor has only a small effect on net CO_2 fluxes as "seen" by the atmosphere (see Section 6.3).

No clear optimum appears with Formulations II, VI and VIII, where SR was set to zero for monthly mean temperatures below -10°CHere, the optimal Q_{10} shifts to unreasonably low values, lies below 1.0 for II and VIII. This leads to a functional form where the seasonality of SR is dominated by the -10°C criterion, which clearly is not observed in the field. If we therefore, reject the idea of a low-temperature cutoff — this will be further discussed in Section 6.4 — we are left with Formulations I and VII, which both have a clear optimum at $Q_{10} = 1.5$, regardless of the wind data used.

Figure 2 shows the observed and simulated seasonal cycle of CO_2 concentration at the stations used for defining the costfunction, J (cf. Table 1), derived from Formulations I and VII with the optimized value for A, and thus glNPP, according to Table 2, but with varying values of Q_{10}. In all cases, 1987 wind data is used. For comparison, results for Cape Grim (CGO) are also shown. At most stations the maximum depletion of CO_2 during summer is poorly matched in the model. We suppose, for CBA and BRW in particular, that this can at least partly be explained by the presence of local vegetation that cannot be adequately represented at the

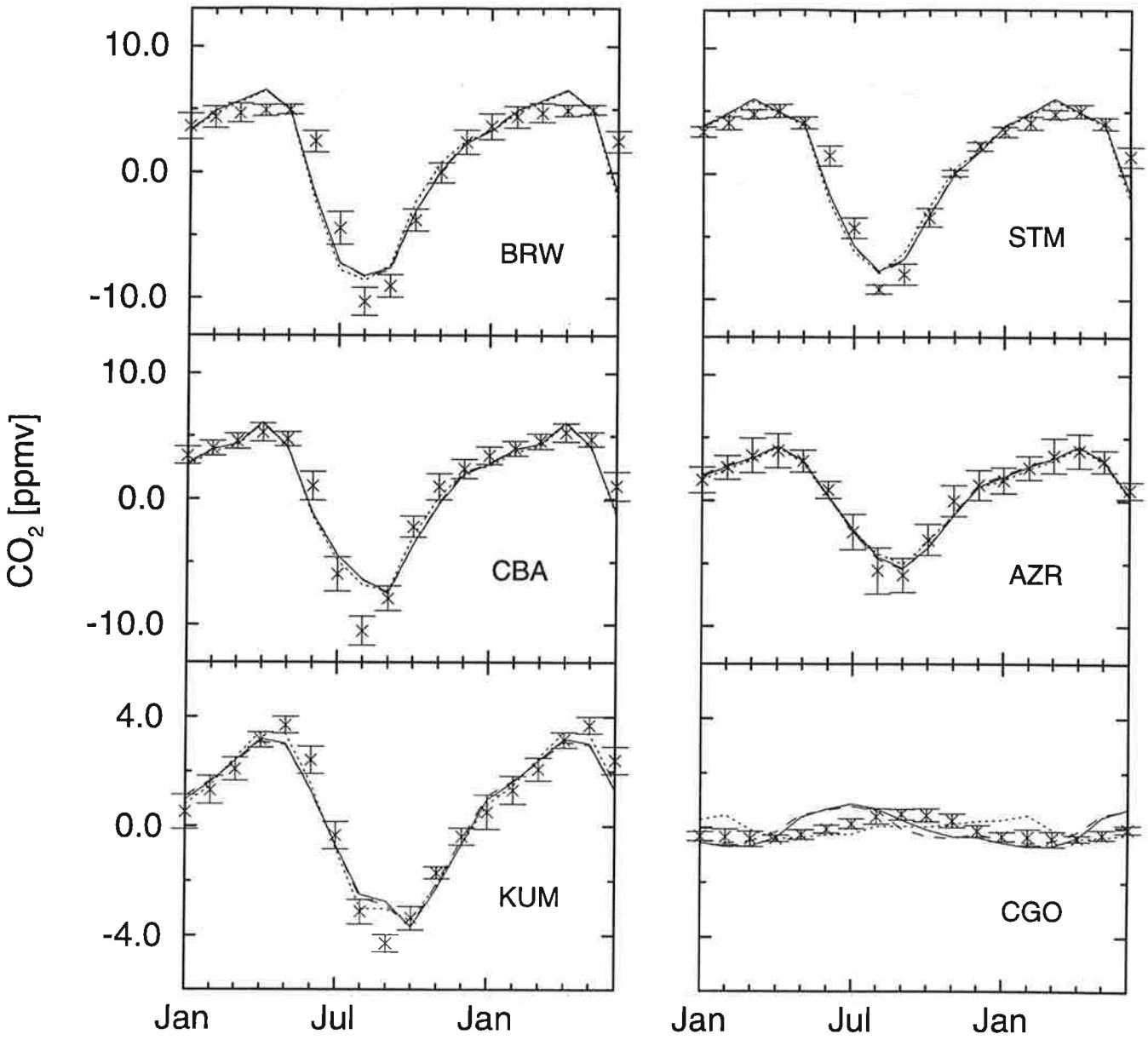

Figure 2: Simulated and observed seasonal cycle at those stations used for calculating the cost function, J, plus Cape Grim (CGO, 41°S, 145°E), for Formulations I (full curve), III (dotted) and VII (dashed) with the respective best-fit values for Q_{10} (all 1.5), using 1987 winds. Observations, $c_{i,obs}$, are shown with error bars indicating $s_{i,obs}$. The first half of the annual cycle is repeated for display purposes.

coarse resolution of the TM2. (Although the biosphere model works at 0.5^o, fluxes are always aggregated to TM2 resolution.) Simulations generally lead observations by up to one month during the spring depletion of CO_2. In part, this is an effect of the monthly NDVI maximization, that has a bias towards choosing values from later in the month when grenness is increasing. However, an additional reason could be high maintanance respiration during spring build-up of vegetation (cf. Section 6.2). In general, differences between the various formulations are small and the curves are often indiscernible.

In addition to simulating the seasonal cycle of CO_2 fluxes, we assess year-to-year variability within the model. Such variability results from changes in the wind data as well as from changes in the NDVI and climate data used to drive the vegetation model. We perform two tests for the years 1986 and 1987, simulating both winds and vegetation activity for that particular year, using Formulation I and $Q_{10} = 1.5$. The results are shown in Figure 3. We have added two runs where the vegetation is driven by the mean climate in order to allow separation of the effect of changing winds alone. In all cases we use the same value for the global photosynthetic efficiency, A, as it was optimized with 1987 winds (0.55 gC/MJ, see below). We find that, in general, observed and simulated year-to-year variability are of roughly the same size. The results suggest that changes in in vegetation activity play a lesser role than changes in atmospheric transport patterns, except for BRW during late summer, probably because of the proximity to local vegetation. The same effects might also cause the year-to-year variability at BRW to be larger than simulated. For comparison we show results for another arctic North American station, Alert on Ellesmere Island (ALT, 62^oW, 83^oN), where local vegetation is almost absent.

The optimized global photosynthetic efficiency, A, for the two best-fit cases is 0.55 gC/MJ (Formulation I, $Q_{10} = 1.5$) and 0.53 gC/MJ (Formulation VII, same Q_{10}; 1 gC $= 10^{-3}$ kg of carbon). Light-use efficience, ϵ, is normally defined through NPP $= \epsilon *$ IPAR where IPAR is that part of PAR that is intercepted by the canopy. The ratio IPAR/PAR is usually denoted FPAR, i.e. fraction of intercepted PAR. According to a theoretical study by Asrar et al. (1992), FPAR is approximately linearly related to NDVI, even for heterogeneous vegetation cover, and complete absorption should occur at a NDVI value of approximately one, i.e. FPAR $\approx$ NDVI. However, despite the monthly maximization that was carried out on the original daily NDVI data, there is still considerable atmospheric contamination reducing the highest values in the data set, assumed to represent complete vegetation cover, to around 0.60. Therefore, we take FPAR = NDVI/0.60. Assuming that PAR is one half of solar radiation, R_S, (Prince 1991) we obtain:

$$\text{NPP} = \epsilon * \text{NDVI}/0.60 * R_S/2 \tag{4}$$

Comparing that to Equations 2a and 2b allows us to translate A into ϵ, and thus we obtain $\epsilon = 0.66$ gC/MJ PAR * AET/PET for Formulation I, and $\epsilon = 0.64$ gC/MJ PAR for Formulation VII. Cited values for natural vegetation range from 0.4 to 3.0 g dry matter/MJ PAR (Running and Hunt 1993), and for crops from 0.8 to 4.8 g dry matter/MJ PAR (Prince 1991), which translates to 0.2 to 1.4 gC/MJ PAR and 0.4 to 2.2 gC/MJ PAR, respectively, assuming 45% carbon content of dry

matter.

For further discussion, it is important to note that most of the seasonal cycle at the stations in Table 1 comes from vegetation north of 23.5°N. The amplitude caused by fluxes from the tropical belt (23.5°N to 23.5°S) only reaches 2.2% of the full simulated seasonal cycle at the southernmost of these stations, Cape Kumukahi, with Formulation I, $Q_{10} = 1.5$. For Formulation VII, same Q_{10}, the figure is 3.7%.

Summarizing, we reject including AET/PET only into NPP (III), or only into SR (V and VI), on the grounds that the amplitude either in southern-temperate or on southern-tropical latitudes is much larger than observed, and a SR cutoff at -10°C (II, VI and VIII), because the optimized functional form defies common experience in the field. The two best fits include AET/PET either into both fluxes (I), or into none of the two (VII). The results appear to be independent of year-to-year changes in atmospheric transport and vegetation activity.

5.2 Additional checks

Prior to the main simulations described in the previous section, we perform a number of data consistency checks. Apart from changing between 1986 and 1987 wind fields, which we have already discussed, they include using monthly vs. biweekly NDVI maxima, monthly vs. interpolated daily flux updates in the TM2, and NDVI vs. Simple Ratio Vegetation Index (i.e. near-infrared divided by red reflectivity). The most significant effect is found when changing from 1987 to 1986 winds (cf. Table 2), with the remaining three tests leading only to small changes in the output data compared to the uncertainty resulting from the choice of the wind data. Therefore, we keep monthly flux updates to the TM2 and monthly maxima of NDVI.

We also test changing the scaling factors for convection and for vertical diffusion both from 1.0 (standard case) to 0.25 (cf. Keeling et al. 1989, Heimann 1994). The effect on vertical transport can be assessed by comparing seasonal cycles at Mauna Loa (MLO), at 3397 m height, to Cape Kumukahi (KUM), at sea level, both on Hawaii. The observed seasonal amplitude at MLO is about $15 \pm 5\%$ smaller than at KUM. In the standard case this difference is 22%, i.e. it is slightly overstressed. However, the difference increases markedly to 36% when the scaling factors are reduced.

6 Discussion

6.1 Model sensitivity

In this systematic exploration of functional forms of atmosphere-biosphere CO_2 exchange we have found a number of good fits to the observed seasonal cycle of atmospheric CO_2. They compare well those achieved in Heimann et al. (1989), and are superior to those in an earlier study be Fung et al. (1987). A good fit is achieved by a range of formulations, which illustrates how underdetermined the inversion of atmospheric transport is, even with the highly constrained model used in this study. Limiting factors are fluctuations in the observed seasonal cycle, changes in the wind

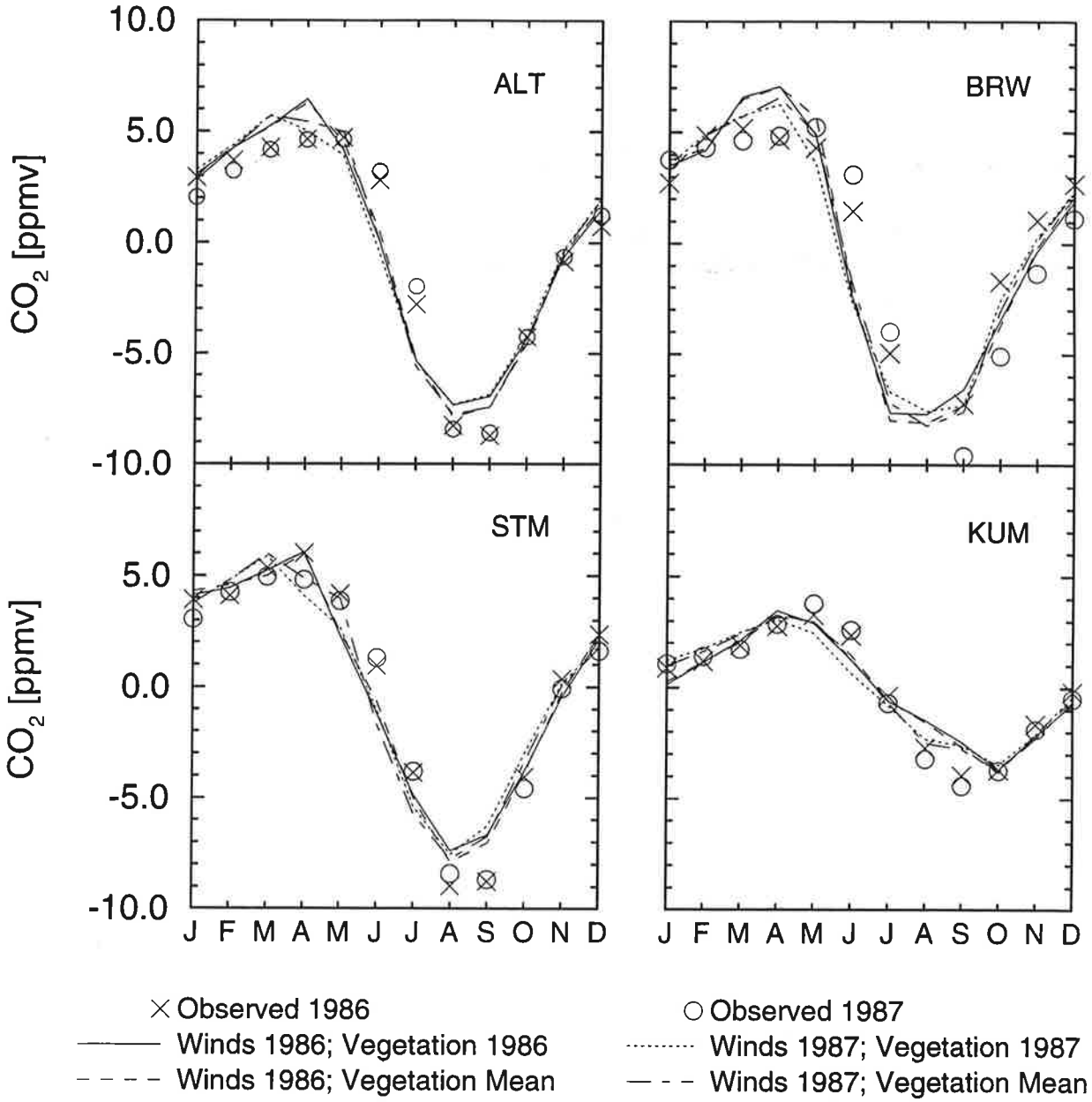

Figure 3: Observed and simulated seasonal cycle of CO_2 with data only from 1986 and 1987, respectively. For comparison, results with simulated vegetation activity using ECMWF and NDVI data from a four-year mean are also shown. In all simulations we take the optimized value from Formulation I for the global photosynthetic efficiency ($A = 0.55$gC/MJ).

data, and uncertainties about non-biospheric contributions. The latter limitation makes it difficult to test assumptions about vegetation activity in the large tropical biomes. Apart from an accurate resolution of the monsoon circulation, accurate data on the ratio of $^{13}CO_2$ to $^{12}CO_2$ could resolve this problem, because this ratio allows the determination of the biospheric contribution to changes in the CO_2 concentration (Keeling et al. 1989). Local-vegetation effects also seem to contribute to discrepancies between observations and simulations. This problem might be hard to overcome, since an adequate resolution of the boundary layer is probably not feasible.

Despite these limitations, however, the simple models developed in this study can be tested and parameters can be tuned accurately enough to draw some cautious conclusions about the physiology of global vegetation (see following subsections). We also find that the year-to-year variability of the seasonal cycle at sufficiently remote stations is roughly of the observed magnitude, and that such variability appears to be dominated by changes in the wind data. This suggests that we could possibly improve the simulation method by running the TM2 over several consecutive years with the actual observed winds.

6.2 Definition of biospheric fluxes

Before discussing physiological conclusions, a closer look at the definition of NPP and SR is appropriate. NPP is commonly defined as total photosynthesis, called Gross Primary Productivity (GPP), minus all autotroph respiration, R_a: NPP = GPP$-R_a$. We have thus far assumed this to be true for this study. We have also assumed to a counterbalancing release of carbon back to the atmosphere, SR, consisting solely of heterotroph respiration from dead plant material, i.e. SR = R_h. Thus we have for annual means:

$$\overline{\mathrm{GPP}} - \overline{R_a} = \overline{R_h} \tag{5}$$

This perfect balance between NPP and SR is a rather strong assumption when considering a particular test sight (cf. Wofsy et al. 1993). However, the largest imbalances will be introduced by management practices and changes in the disturbance regime (Kurz et al. 1992, Wofsy et al. 1993), and these will be too long-term to have any significant effect on the seasonal cycle.

Estimates for global annual NPP range from 47 GtC (Whittaker and Likens, 1973, Lieth 1975; 1 GtC = 10^{12} kg of carbon) to 60 GtC (Ajtay et al. 1979, Olson et al. 1983). Taking our current definition of NPP given, annual NPP can be equated with annual plant detritus production, equivalent to $\overline{R_h}$. This was estimated by Meentemeyer et al. (1982) at 55 GtC globally. The term $\overline{R_a}$ in Equation 5 can be further separated into contributions from aboveground vegetation, R_a^{above}, and roots, R_a^{root}. The latter is hard to separate from R_h when measuring soil release. Therefore, Raich and Schlesinger (1992) give a global estimate of total soil release, including root respiration, i.e. of R_h plus R_a^{root}, of 68 GtC annually. They also find that this quantity is, for the major biomes, on average around 24% higher than NPP and thus arrive at an estimate of 55 GtC for glNPP.

It is important to note that the time step implied in the NPP data cited above is one year, with the build-up and shedding of leaves and fruits undergoing a yearly

cycle, apart from some evergreen tropical vegetation. At this time scale, autotroph respiration can be excluded from net fluxes. At the other extreme, at a sub-daily time scale autotroph maintenance respiration would have to be accounted for explicitly in order to simulate the diurnal cycle of CO_2 fluxes. In this way the inherent time scale determines what a net flux is. Consequently, we separate autotroph respiration, R_a, into a fast, R_a^f, and a slow component, R_a^s. Fast in this context means that resisdence time of carbon is less or equal to the basic model time step. (R_h is considered entirely slow.) That leads us to a new, time-scale dependent definition of NPP and SR: NPP = GPP $- R_a^f$ and SR = $R_h + R_a^s$. Thus, the annual balance becomes:

$$\overline{\mathrm{GPP}} - \overline{R_a^f} = \overline{R_h} + \overline{R_h^s} \tag{6}$$

Since autotroph respiration that is out of phase with photosynthesis, i.e. R_a^s, will show up in atmospheric transport, this definition is probably more appropriate for our model. The difficulty, however, lies in the fact that autotroph and heterotroph respiration, both now included into SR, have a different functional dependence on environmental factors. A solution would be to parameterize R_a^f R_a^s explicitly. In the context of this study, however, this would unnecessarily complicate the model. Therefore, the question remains how large the difference between the two definitions of NPP is for our monthly biosphere model.

In fact, during most of the vegetation period carbon loss through autotroph respiration will be covered immediately by gains from day-time photosynthesis, so that the difference will be small. We expect that the main contribution to R_a^s will come from stem respiration during winter and from the build-up of leaves during spring, when maintenance respiration exceeds photosynthetic gain. This spring build-up could also be the reason for the phase lag of observations against simulations in Figure 2 (cf. Section 5.1). In both cases respiration loss of carbon has to be compensated by the depletion of assimilates that were produced during the previous vegetation period. With about 10 GtC annual NPP allocated to temperate and boreal forests and woodlands (Olson et al. 1983), a rough guess for the amount of stem respiration would be 1 to 2 GtC. If we assume 20 GtC for total northern non-tropical NPP, spring build-up could contribute something of a similar size, so that we expect that *by definition* glNPP in our model will exceed cited values by a few GtC. However, a detailed study of the effect of time scale on net flux sizes would be necessary for a proper assessment.

6.3 Impact of water stress

It is important to note that almost all the signal used for fitting originates from northern temperate and boreal vegetation. Comparing the three best fits from Table 2, shown in Figure 2, reveals no marked differences in the simulated seasonal cycles at northern-hemisphere stations. Notably, even Formulation III, with a much different southern-hemisphere seasonality, could pass as a good fit when looking only at the stations shown in Figure 2, because the simulated signal at CGO has roughly the same amplitude as the observed one. However, as discussed in Section 5.1, III can be excluded by considering also CO_2 measurements from Ascension Island. This shows

how important it is to have a network of remote monitoring sites that spans much of the globe, as provided by the NOAA/GMCC flask sampling network (Conway and Tans, 1990).

At the northern-hemisphere stations used for fitting global parameters the difference between the three formulations is very small. In the case of Formulations I and VII, the two curves are almost indiscernable. The reason for this is that drought stress, quantified as AET/PET, has only a relatively small effect on northern vegetation, mainly during the summer months. This can be seen in Figure 4 on Graphs (b) and (d), reprenting tundra and evergreen needle-leaved forest, respectively. (We have chosen to show Formulation VIII instead of VII to demonstrate the effect of a low-temperature cutoff as well, cf. next subsection). In addition, Formulation I reduces both CO_2 uptake and release simultaneously by the same factor, AET/PET, so that there is only a small difference in the net flux compared to Formulation VII, where no drought-stress factor is applied at all. Formulations I and VII are also the ones that pass the test at the CGO and ASC.

For the tropical belt, the inclusion of a drought-stress factor matters far more than for the extratropics. This can be seen on Figure 1 for ASC, where much of the signal comes from tropical vegetation south of the equator. One such area is represented by Graph c in Figure 4. Both figures show that the simulated net seasonal CO_2 exchange differs vastly between the different model formulations used. (Evidently, the low-temperature cutoff has no influence in these areas so that e.g. VII and VIII are identical.) The easiest to interprete is Formulation VII. Here, CO_2 release is nearly constant over the year, whereas CO_2 uptake declines during the dry season because of a decline in the NDVI. This decline in NDVI is, however, much less pronounced than the decline in the drought-stress factor, AET/PET, which goes to near-zero in the area represented in Figure 4, Graph c. Consequently, for Formulation III, with the same SR but the additional drought-stress factor in NPP, seasonal CO_2 exchange has about the same phase but a markedly larger amplitude. The dominant role of the factor AET/PET also causes Formulation V to produce a seasonal cycle of just the opposite orientation as III or VII, because in this case SR declines to almost zero during the dry season, while NPP is only reduced to around half its peak value, making the dry season a period of net CO_2 uptake. Finally, with Formulation I we simulate only a very small seasonal net CO_2 exchange, because the drought-stress factor reduces SR and NPP simultaneously.

Comparing simulations with observations (see Figure 4), with all the limitations mentioned in Section 4.1, it seems that only Formulation I, which produces a very small seasonal CO_2 exchange in the tropics, can edaquately represent tropical vegetation activity. It appears that even Formulation VII produces too large a seasonal cycle at ASC, although this is not obvious enough for a rejection. Our conclusion for tropcial vegetation is that CO_2 uptake and release happen mostly simultaneously, reducing net exchange considerably compared to temperate and boreal vegetation.

It is instructive to consider the global values of Growing Season Net Flux (GSNF), defined as the sum of the monthly net CO_2 exchange as long as net flux goes into the vegetation at one particular grid cell. As expected, this value is highest for III and V (both 14.5 GtC), less for VII (12.5 GtC), and smallest for I (10.2 GtC).

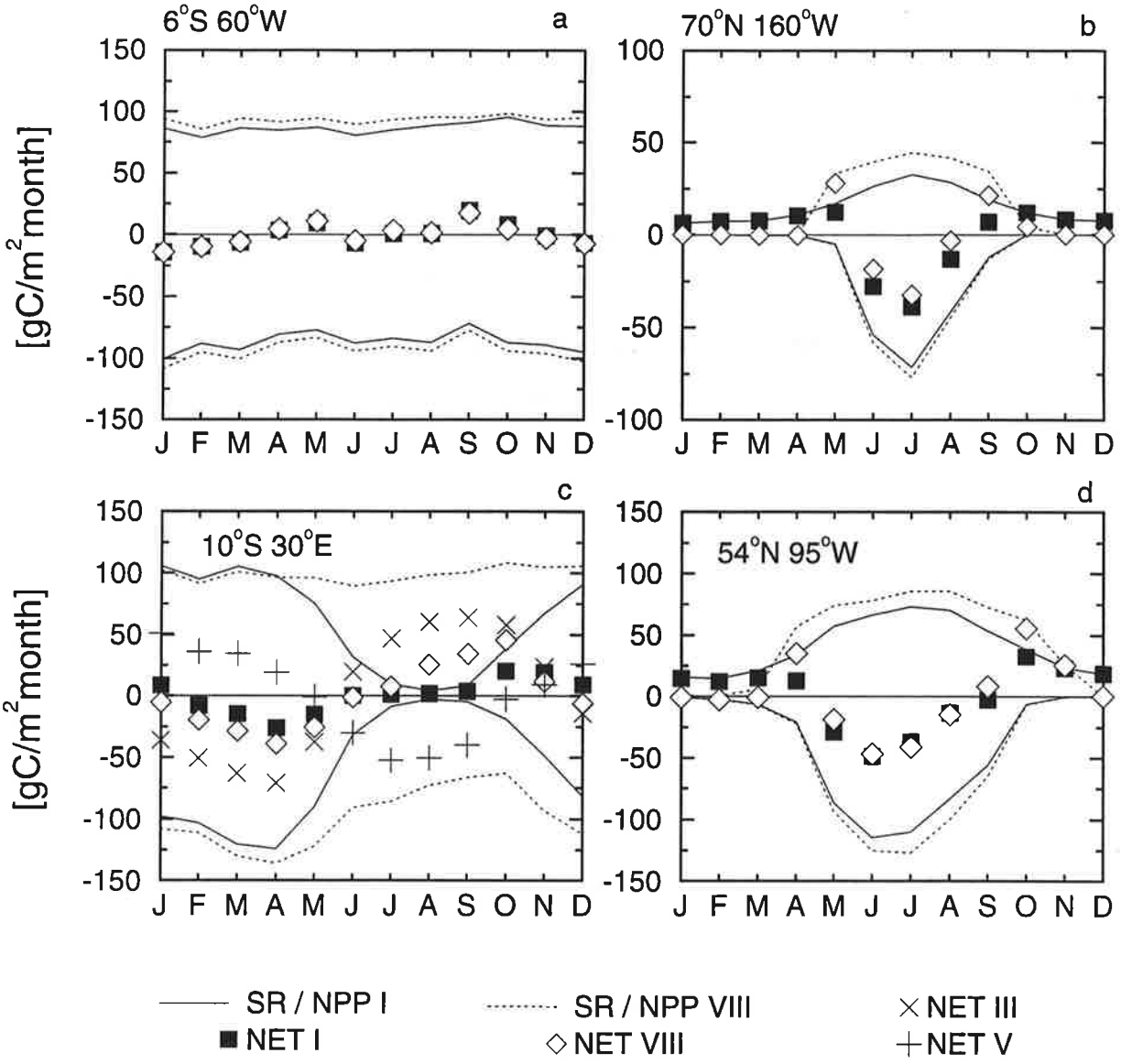

Figure 4: Monthly carbon fluxes – SR (> 0); NPP (< 0); net flux (NET) – from four grid boxes of 4^o latitude by 5^o longitude for Formulations I, $Q_{10} = 1.5$, and VIII, $Q_{10} = 1.2$. VIII was chosen instead of VII to show the effect of both the low-temperature cutoff during winter, and the drought-stress factor mainly during the summer, in Graphs (b) to (d). For easy comparison, all grid boxes except (c) are identical to those displayed in Fung et al. (1987). Grid boxes are dominated by (a) rain forest; (b) tundra; (c) drought-deciduous woodland; and (d) evergreen needle-leaved forest (Matthews 1983). Coordinates of the grid box centres are indicated in the figure. Note that the photosynthetic efficiency, A, is not the same for I and VIII.

The differences come almost entirely from tropical regions, begause drought stress is only small in areas of temperate or boreal vegetation.

However, it is not only tropical summer-rain, but also subtropical winter-rain vegetation that experiences large seasonal drought stress. Such areas are abundant in subtropical Australia, and we suggest that the apparent mismatch at CGO between observations and simulations with Formulation V can be explained by the fact that the impact of drought on such vegetation is inadequately represented. In fact, in a seperate simulation we find that about 80% of the simulated amplitude at CGO comes from vegetation south of the Tropic of Capricorn when using Formulation V. In this case, SR dominates during the humid winter, whereas NPP is overestimated during the mainly dry summer because drought stress of plants is neglected. The resulting net CO_2 flux has the same seasonality as the flux from temperate vegetation, so that the two signals largely add up. This causes the simulated amplitude at CGO to be much too large. It seems that, as in the case of tropical summer-rain vegetation, both CO_2 uptake and release largely happen simultaneously so that both Formulation I and VII produce satisfactory results.

Apparently, although Formulation I seems to be performing somewhat better at ASC than VII, it is not possible to decide definitely whether to include AET/PET into both NPP and SR or none of the two on the basis of atmospheric transport and observed CO_2 alone. Obviously, there must be *some* dependence on drought stress of both NPP and SR, but inversion of atmospheric transport will not be able to determine this dependence. This is because in those areas where drought stress matters most, net fluxes appear to be small. However, we know from physiology that forests, contributing most to NPP globally (Olson et al. 1983), respond to water pressure deficit by stomatal closure. Since this is not visible in the NDVI, it would be necessary to account for the response of forests to drought stress explicitly in NPP, as it is done in Formulation I. In fact, independent estimates of global NPP seem to favour Formulation I, although it is hard to quantify whether the more 'realistic' NPP value outweighs the inferior cost function. We therefore compare annual NPP for Formulations I and VII with a global NPP map by Fung et al. (1983) on the same 7.83 by 10.00 degree grid of the TM2, based on the global vegetation map by Matthews (1983). The comparison, restricted to grid cells with at least 50% land cover, is displayed in Figure 5. The global total for the Fung et al. data (45 GtC) is significanctly smaller than the corresponding values in our study (63 and 78 GtC, cf. Table 2). Nontheless, the correlation of all displayed data points is considerable (I: 0.88; VII: 0.86, number of data points: 201).

This good agreement is encouraging, because both data sets were generated using complementary concepts. Whereas our study assumes that NPP is solely controlled by environmental factors, the Fung et al. data have been generated by assigning the same annual NPP to each vegetation type, based on field studies, and then using a global vegetation map (Matthews 1983). In particular, there is no systematic overestimate of NPP in the tropics, although we have ignored any temperature dependence of NPP. (Higher temperatures usually imply higher maintenance respiration, thus reducing NPP and therewith the photosynthetic efficiency, A, which we have assumed globally constant.)

However, for the tropical latitudes (15.65°S to 15.65°N, represented by the larger black dots in Figure 5), the agreement is visibly superior for Formulation I against Formulation VII (correlation coefficient, I: 0.86; VII: 0.68; number of data points: 28). This is because Formulation VII assigns broadly the same annual NPP (around 1000 gC/m^2) to large areas of the tropics, whereas the same areas show a much larger variability in annual NPP both with Formulation I and in the Fung et al. data. In the Matthews vegetation map, these areas are assigned to tropical rainforest, tropical drought-deciduous woodland, grassland with 10 to 40% tree cover, and xeromorphic forest/woodland. There are no significant differences in the annual mean NDVI, hence the uniformity of annual NPP with Formulation VII. In contrast, Fung et al. assume 945 gC/m^2 for tropical rainforest, and values around 300 gC/m^2 for the remaining vegetation classes. Such a decline in productivity when going from the equatorial rain forest to the adjacent drought affected regions can also be seen in the data produced with Formulation I, which additionally accounts for variations in rainfall; hence the good agreement between Formulation I and the Fung et al. data. On the other hand, around the Tropic of Cancer we find a number of grid points where Formulation I derives annual NPP below 10^{10} kgC per TM2 grid cell, whereas Matthews-based values are significantly higher (see the plus signs in Figure 5, upper graph). For those arid regions, the agreement is clearly better with Formulation VII. Possible explanations include insufficient precipiation data, and inadequate representation of sparse desert vegetation in the Matthews-Fung model, where Sahel grasslands are assigned the same annual NPP as e.g. grasslands in southern Brazil.

As stated in Section 4.2, we expect Equation 2a to be more appropriate for forests, and Equation 2b to be better suited for grasslands and arid regions, where vegetation quickly responds to rainfall. This assumption is supported by the comparisons made in the preceding paragraph. Given that globally forests and woodlands contribute much more to NPP than grasslands (Olson et al. 1983), we find that Formulation I is more suited for a global-scale model. We also find some evidence that the seasonal cycle of CO_2 exchange in the tropics is more adequately represented by I than by VII. Furthermore, Formulation VII appears to overestimate global NPP because it fails to reproduce the reduction in NPP of drought stressed forests. Since the global photosynthetic efficiency, A, comes out roughly the same in both formulations, we might thus interpret the difference in glNPP, 16 GtC, mainly in the tropics, as the size of the decline in NPP globally resulting from water deficit. This value increases to 18 GtC if we use the same value for A in VII as in I, 0.55 gC/MJ. We therefore conclude that Formulation I is probably most adequate for a globally uniform model of vegetation functioning.

6.4 Winter-time CO_2 release

In contrast to the preceding subsection, it is much easier to decide against setting Q_{10} to zero at low freezing temperatures from CO_2 observations and atmospheric transport modelling alone. Our results suggest that there is considerable release of carbon from vegetation out of phase with NPP, i.e. during the winter months. A low-temperature cutoff reduces those fluxes to early spring and early winter, requiring

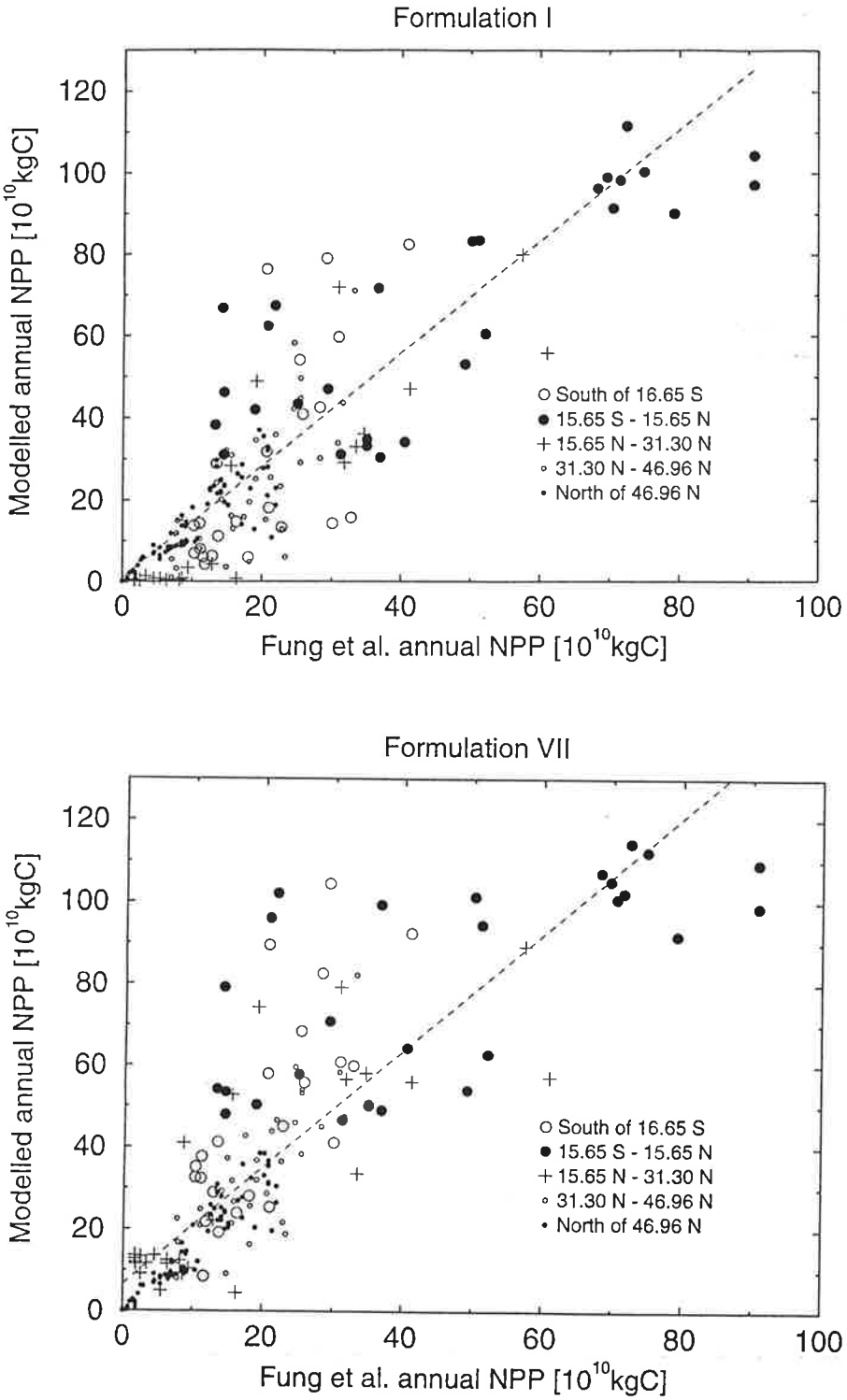

Figure 5: Comparison of the annual NPP at the TM2 resolution from Formulation I (upper graph) and Formulation VII (lower graph) against values by Fung et al. (1983) based on a vegetation map by Matthews (1983). We exclude all grid cells with less than 50% land cover. A linear regression of all data points is indicated by a dashed line.

either an unreasonably high NPP, or an unreasonably low Q_{10}, since temperatures are still low at that time. In the study by Fung et al. (1987) SR was assumed to increase linearly with temperature, and to cease below a value of -14.3°C for temperate or boreal needle-leaved vegetation, and -6.25°C for temperate or boreal broad-leaved vegetation. In Figure 4 we show fluxes from various grid boxes identical to those used in the Fung et al. study for Formulation I ($Q_{10} = 1.5$) and VIII ($Q_{10} = 1.2$). The latter corresponds to the one used in Heimann et al. (1989), except that they use a Q_{10} of 1.5. Fluxes for Formulation VIII are also similar to those derived by Fung et al., where the Q_{10} implied in going from 0°C to 10°C is 1.9 and 2.4, respectively, i.e. much larger than the optimal value found in our study when using a cutoff. In fact, in the study be Fung et al. the simulated seasonal CO_2 concentration at Point Barrow, Alaska, is clearly too low during winter, which could well be attributed to missing winter-time CO_2 release.

We therefore conclude that there must be a considerable amount of CO_2 released from soils during the winter. This is supported by the results of a number of field studies, where litter decomposition proceeded with no significant slowdown under snow cover (Moore 1983, Stohlgren 1988, Taylor and Jones 1990). The heat insulating property of snow left the soil relatively warm at 0 to -3°C compared to air temperatures down to -35°C (Moore 1983). The CO_2 produced during litter decay probably escapes fast enough to show up in atmospheric transport as winter-time release. This was found by Solomon and Cerling (1987) who measured CO_2 concentrations within soil and snowpack in a montane environment in Utah. However, the field studies mentioned are from sites with a large amount of snowfall compared to the more continental climates of e.g. the Siberian boreal forest areas. Nonetheless, a smaller amount of snow cover in those latter regions might still be a sufficient insulator to favour bacterial activity, but be even better at letting CO_2 escape to the atmosphere.

7 Conclusions

In this study we have investigated what insights can be gained from testing a biosphere model by coupling CO_2 fluxes to an atmospheric tracer transport model and checking results against observations. The overall picture is that such an inversion is highly underdetermined with regard to the functional dependence of biosphere-atmosphere CO_2 exchange. This is largely because uptake and release of CO_2 often happen in phase, so that the net flux to the atmosphere is small compared to the amount of carbon cycled locally. Year-to-year changes in atmospheric transport introduce a further difficulty. However, when constraining the biosphere model to a small number of parameters, some clear trends are visible. We have found a number of indications of the importance of including water availability, and the results point strongly towards a considerable carbon release from soils during northern-hemisphere winter.

By deliberately simplifying our biosphere model to a minimum number of parameters, we have been able to explore systematically a wide range of model formu-

lations and parameter settings. Thus we have found a formulation that goes beyond those used previously in similar studies (Fung et al. 1983, 1987; Heimann and Keeling 1989) by taking account of water availability. However, the method can equally be used to test more complex, mechanistic terrestrial ecosystem models. This study should give an idea of the scope as well as the limitations of such a test.

It would be a significant step forward to simulate interannual fluctuations of atmospheric CO_2 in the same way as it has been done for the seasonal cycle. Such fluctuations appear to be linked to the El Niño-Southern Oscillation (Keeling et al. 1989), and possibly to violent volcanic eruptions, such as the recent one of Mount Pinatubo (Sarmiento 1993). This requires extremely accurate measurements of the carbon isotope ratio of atmospheric CO_2 to extract the biospheric contribution to CO_2 variations. Such data are not yet available for longer periods. Further, both the vegetation index and the meteorological data we have used contain inhomogeneities and trends that, because of the delicate balance between carbon uptake and release, dominate interannual carbon flux variations when we run our model interannually. Significant improvements concerning data quality are therefore needed. With such improvements, however, it would be most instructive to compare interannual fluctuations in atmospheric CO_2 derived taking a range of model formulations used in this study with those calculated with a number of existing terrestrial ecosystem models.

8 Acknowledgements

The authors wish to thank Alex Haxeltine, Jörg Kaduk, Bettina Loth and Ramakrishna Nemani for helpful discussions, and Gérard Dedieu for reviewing the original manuscript. The ECMWF data were obtained through Deutscher Wetterdienst, Offenbach, Germany. This work has been funded in part by the European Commission under Contract No. EV5V-CT92-0120.

References

Ajtay, G.L., Ketner. P. and Duvigneaud, P. 1979. Terrestrial primary production and phytomass. In: *The Global Carbon Cycle* (eds. B. Bolin, E.T. Degens, S. Kempe and P. Ketner). New York: John Wiley. 129-181.

Arpe, K. 1991. The hydrological cycle in the ECMWF short range forecasts. *Dyn. Atmos. Oceans 16*. 33-59.

Asrar G., Fuchs, M., Kanemasu, E.T. and Hatfield, J.L. 1984. Estimating absorbed photosynthetically active radiation and leaf area index from spectral reflectance in wheat. *Agronomy J. 76*, 300-306.

Asrar, G., Myneni, R.B. and Choudhury, B.J. 1992. Spatial heterogeneity in vegetation canopies and remote sensing of absorbed photosynthetically active radiation: a modeling study. *Remote Sens. Environ. 41*, 85-103.

Bonan, G.B., 1991. Atmosphere-biosphere exchange of carbon dioxide in boreal forests. *J. Geophys. Res. 96*, 7301-7312.

CDIAC 1991. *Trends 1991, a compendium of data on global change* (eds. T.A. Boden, R.J. Serpanski and F.W. Stoss). Oak Ridge/Tennessee: ORNL/CDIAC-46, Carbon Dioxide Information Center, Oak Ridge National Laboratory.

Conway, T.J. and Tans, P. 1990. *Atmospheric CO_2 concentrations — The NOAA/GMCC flask sampling network.* Oak Ridge/Tennessee: NDP-005/R1, Carbon Dioxide Information Center, Oak Ridge National Laboratory.

Enting, I.G. and Mansbridge, J.V. 1989. Seasonal sources and sinks of atmospheric CO_2: direct inversion of filtered data. *Tellus 41 B*, 111-126.

Enting, I.G. and Mansbridge, J.V. 1991. Latitudinal distribution of sources and sinks of CO_2: results of an inversion study. *Tellus 43 B*, 156-170.

Fung, I., Prentice, K., Matthews, E., Lerner, J. and Russel, G. 1983. Three-dimensional tracer model study of atmospheric CO_2: Response to seasonal exchanges with the terrestrial biosphere. *J. Geophys. Res. 88*, 1281-1294.

Fung, I.Y., Tucker, C.J. and Prentice, K.C. 1987. Application of advanced very high resolution radiometer vegetation index to study atmosphere-biosphere exchange of CO_2. *J. Geophys. Res. 92*, 2999-3015.

Gallo, K.P. 1992. *Experimental global vegetation index from AVHRR utilizing pre-launch calibration, cloud and sun-angle screening.* Digital Data. Boulder/Colorado: National Oceanic and Atmospheric Administration, National Geophysical Data Center.

Gao W., Wesely, M.L., Cook, D.R. and Hart, R.L. 1992. Air-surface exchange of H_2O, CO_2 , and O_3 at a tallgrass prairie in relation to remotely sensed vegetation indices. *J. Geophys. Res. 97*, 18663-18671.

Goward, S.G., Tucker, C.J., Dye, D.G. 1985. North American vegetation patterns observed with the NOAA-7 advanced very high resolution radiometer, *Vegetatio 64*, 3-14.

Heimann M., 1994. *The TM2 atmospheric transport model.* Hamburg/Germany: Deutsches Klimarechenzentrum Technical Report, forthcoming.

Heimann M. and Keeling, C.D. 1989. A three-dimensional model of atmospheric CO_2 transport based on observed winds: 2. Model description and simulated tracer experiments. *AGU Monograph 55.* Washington, American Geophysical Union. 237-275.

Heimann M., Keeling, C.D. and Tucker, C.J. 1989: A three-dimensional model of atmospheric CO_2 transport based on observed winds: 3. Seasonal cycle and synoptic time scale variations. *AGU Monograph 55.* Washington, American Geophysical Union. 277-303.

Janacek, A., Lüdeke, M.K.B., Kindermann, J. Lang, T.L., Klaudius, A., Otto, R.D., Badeck, F.W. and Kohlmaier, G.H. 1991. A global high resolution mechanistic and prognostic model for the seasonal and long term CO_2 exchange between the terrestrial ecosystems and the atmosphere - The Frankfurt Biosphere Model (FBM). Paper presented at the *3rd International Environmental Chemistry Congress* in Salvador-Bahia, Brazil.

Keeling, C.D., Bacastow, R.B., Carter, A.F., Piper, S.C., Whorf, T.P., Heimann, M., Mook, W.G. and Roeloffzen, H. 1989. A three-dimensional model of atmospheric CO_2 transport based on observed winds: 1. Analysis of observational data. *AGU Monograph 55.* Washington, American Geophysical Union. 277-303.

Kumar, M. and Monteith, J.L. 1981: Remote sensing of crop growth. In *Plants and the Daylight Spectrum* (ed. H. Smith). London: Academic Press, 133-144.

Kurz, W.A., Apps, M.J., Webb, T.M. and McNamee, P.J. 1992. *The carbon budget of the Canadian forest sector: Phase I.* Edmonton/Canada: Information Report NOR-X-326, Forestry Canada.

Lieth, H., 1975. Primary production of the major vegetation units of the world. In *Primary productivity of the biosphere* (eds. H. Lieth and R.H. Whittaker). New York: Springer Verlag.

Matthews, E., 1983: Global vegetation and land use: A new high-resolution data base for climate studies, *J. App. Meteorol. 22*, 474-487.

Meentemeyer, V., 1978. Macroclimate and lignin control of litter decomposition rates, *Ecology 59*, 465-472.

Melillo J.M., McGuire, A.D., Kicklighter, D.W., Moore III, B., Vörösmarty, C.J. and Schloss, A.L. 1993: Global climate change and terrestrial net primary production, *Nature 363*, 234-240.

Monteith, J.L., 1977. Climate and the efficiency of crop production in Britain. *Philosophical Transaction of the Royal Society of London B281*, 277-294.

Moore, T.R., 1983. Winter-time decomposition in a subarctic woodland. *Arct. Alp. Res. 15*, 413-418.

Myneni, R.B., Ganapol, B.D. and Asrar, G. 1992. Remote sensing of vegetation canopy photosynthetic and stomatal conductance efficiences. *Remote Sens. Environ. 42*, 217-238.

Nakazawa, T., Morimoto, S., Aoki, S. and Tanaka, M. 1993. Time and space variations of the carbon isotopic ratio of tropospheric carbon dioxide over Japan. *Tellus 45 B*, 258-274.

Norman, J.M., Garcia, R. and Verma, S.B. 1992. Soil surface CO_2 fluxes and the carbon budget of a grassland. *J. Geophys. Res. 97*, 18845-18853.

Olson, J.S., Watts, J.A. and Allison, L.J. 1983. *Carbon in live vegetation of major world ecosystems.* Oak Ridge/Tennessee: Environmental Sciences Division Publication Number 1997.

Prentice, I.C., Sykes, M.T., and Kramer, W. 1993. A simulation model for the transient effects of climate change on forest landscapes, *Ecol. Modelling 65*, 51-70.

Raich, J.W. and Schlesinger, W.H. 1992. The global carbon dioxide flux in soil respiration and its relationship to vegetation and climate. *Tellus 44 B*, 81-99.

Raich, J.W., Rastetter, E.B., Melillo, J.M., Kicklighter, D.W., Steudler, P.A., Peterson, B.J., Grace, A.L., Moore III, B. and Vörösmarty, C.J. 1991. Potential net primary productivity in South America: application of a global model. *Ecol. Applic. 1*, 399-429.

Running, S.W. 1992. A bottom-up evolution of terrestrial ecosystem modeling theory, and ideas towards global vegetation modeling. In *Modeling the earth system* (ed. D. Ojima). Boulder/Colorado: UCAR/Office for Interdisciplinary Earth Studies.

Running, S.W., and Hunt Jr., E.R. 1993. Generalization of a forest ecosystem model for other biomes, BIOME-BGC, and an application for global-scale model. In *Scaling processes between leaf and landscape levels* (eds. J.R. Ehlinger and C. Field). New York: Springer Verlag.

Running, S.W. and Nemani, R.R. 1988. Relating seasonal patterns of the AVHRR vegetation index to simulated photosynthesis and transpiration of forests in different climates. *Remote Sens. Env. 24*, 347-367.

Sarmiento, J.L. 1993. Atmospheric CO_2 stalled. *Nature 365*, 697-698.

Solomon, D.K. and Cerling, T.E., 1987. The annual carbon dioxide cycle in a montane soil: observations, modeling, and implications for weathering. *Water Resour. Res. 23*, 2257-2265.

Stohlgren, T.J. 1988. Litter dynamics in two Sierran mixed conifer forests. I. Litterfall and decomposition rates. *Can. J. For. Res. 18*, 1127-1135.

Taylor, B.R. and Jones, H.G. 1990. Litter decomposition under snow cover in a balsam fir forest, *Can. J. Bot. 68*, 112-120.

Tucker, C.J. and Sellers, P.J. 1986. Satellite remote sensing of primary production. *Int. J. Remote Sensing 7*, 1395-1416.

Vogt, K.A., Edmonds, R.L., Antos, G.C. and Vogt, D.J. 1980. Relationships between CO_2 evolution, ATP concentrations and decomposition in four forest ecosystems in western Washington. *Oikos 35*, 72-79.

Wofsy S.C., Goulden, M.L., Munger, J.W., Fan, S.-M., Bakwin, P.S., Daube, B.C., Bassow, S.L., Bazzaz, F.A. 1993. Net exchange of CO_2 in a mid-latitude forest. *Science 260*, 1314-1317.

Whittaker, R.H. and Likens, G.E. 1973. Carbon in the biota. In *Carbon and the biosphere* (eds. G.M. Woodwell and E.V. Pecan). Springfield/Virginia: CONF 720510, U.S. National Technical Information Service. 281-302.

MPI Report-Reference: *Reprinted in

Report No. 1-75 Please order the reference list from the MPI Hamburg

Report No. 76
January 1992
A Hybrid Coupled Tropical Atmosphere Ocean Model: Sensitivities and Hindcast Skill
Richard Kleeman, Mojib Latif, Moritz Flügel

Report No. 77
January 1992
A Direct Mathematical Approach to Optimize the Age-Depth Relation of Deep-Sea Sediment Cores
Wolfgang Brüggemann

Report No. 78
January 1992
The Joint Normal Modes of the coupled Atmosphere-Ocean System observed from 1967 to 1986
Jin-Song Xu
* Journal of Climate, 6, 816-838, 1993

Report No. 79
January 1992
Orbital tuning of marine sedimentary cores: An automatic procedure based on a general linear model
Björn Grieger

Report No. 80
March 1992
Application of ocean models for the interpretation of AGCM experiments on the climate of the last glacial maximum
Michael Lautenschlager, Uwe Mikolajewicz, Ernst Maier-Reimer, Christoph Heinze
* Paleoceanography, 7, 769-782, 1992

Report No. 81
March 1992
Normal Modes of the Atmosphere as estimated by Principal Oscillation Patterns and derived from Quasi-Geostrophic Theory
Reiner Schnur, Gerhard Schmitz, Norbert Grieger, Hans von Storch
* Journal of Atmospheric Science, 50, 2386-2400, 1993

Report No. 82
May 1992
On regional surface fluxes over partly forested areas
Martin Claussen, Wim Klaassen
* Beitr. Phys. Atmosph., Vol. 65, 243-248, 1992

Report No. 83
May 1992
On the cold start problem in transient simulations with coupled atmosphere-ocean models
Klaus Hasselmann, Robert Sausen, Ernst Maier-Reimer, Reinhard Voss

Report No. 84
May 1992
Iron fertilization of the Austral Ocean - a model assessment
Katharina D. Kurz, Ernst Maier-Reimer
* Global Biogeochemical Cycles, 7, 229-244, 1993

Report No. 85
June 1992
A snow cover model for global climatic simulations
Bettina Loth, Hans F. Graf, Josef M. Oberhuber
* Journal of Geophysical Research, 98, D6, 10451-10464, 1993

Report No. 86
June 1992
Complex principal oscillation pattern analysis
Gerd Bürger
* Journal of Climate, 1993

MPI-Report-Reference: *Reprinted in

Report No. 87
August 1992
Scale aggregation in semi-smooth flow
Martin Claussen

Report No. 88
August 1992
Optimal fingerprints for the detection of time dependent climate change
Klaus Hasselmann
* Journal of Climate, 6, 1957-1971, 1993

Report No. 89
September 1992
Biomes computed from simulated climatologies
Martin Claussen, Monika Esch
* Climate Dynamics, 9, 235-243, 1994

Report No. 90
September 1992
New generation of radiation budget measurements from space and their use in climate modelling and diagnostic studies
L.Dümenil, E. Raschke

Report No. 91
September 1992
Modal structure of variations in the tropic climate system Part I: Observations
Mojib Latif, Timothy P. Barnett, Keisuke Mizuno

Report No. 92
October 1992
The Köppen Climate Classification as a Diagnostic Tool for General Circulation Models
Ulrike Lohmann, Robert Sausen, Lennart Bengtsson, Ulrich Cubasch
Jan Perlwitz, Erich Roeckner
* Climate Research, 3, 177-193, 1993

Report No. 93
October 1992
Simulation of the present-day climate with the ECHAM model: Impact of model physics and resolution
E. Roeckner, K. Arpe, L. Bengtsson, S. Brinkop, L. Dümenil,
M. Esch, E. Kirk, F. Lunkeit, M. Ponater, B. Rockel, R. Sausen,
U. Schlese, S. Schubert, M. Windelband

Report No. 94
October 1992
Pinatubo Eruption Winter Climate Effects: Model Versus Observations
Hans-F. Graf, Ingo Kirchner, Alan Robock, Ingrid Schult
*Climate Dynamics, 9, 81-93, 1993

Report No. 95
November 1992
A new Atmospheric Surface-Layer Scheme for a Large-Scale Sea-Ice Model
Achim Stössel, Martin Claussen
* Climate Dynamics, 9, 71-80,1993

Report No. 96
December 1992
Modal structure of variations in the tropical climate system Part II: Origins of the Low-Frequency Mode
Timothy P. Barnett, Mojib Latif, Nicholas E. Graham, Moritz Flügel

Report No. 97
December 1992
Monte Carlo Climate Change Forecasts with a Global Coupled Ocean-Atmosphere Model
U. Cubasch, B. D. Santer, A. Hellbach, G. Hegerl, H. Höck
E. Maier-Reimer, U. Mikolajewicz, A. Stössel, R. Voss

Report No. 98
January 1993
Signal-to-Noise Analysis of Time-Dependent Greenhouse Warming Experiments. Part 1: Pattern Analysis
Benjamin D. Santer, Wolfgang Brüggemann, Ulrich Cubasch, Klaus Hasselmann,
Heinke Höck, Ernst Maier-Reimer, Uwe Mikolajewicz

MPI-Report-Reference: *Reprinted in

Report No. 99
January 1993
Locally Modified Bott-Scheme for Highly Convective Flows
Andreas Chlond
* Monthly Weather Review

Report No. 100
March 1993
Discharge data from 50 selected rivers for GCM validation
L. Dümenil, K. Isele, H.-J. Liebscher, U. Schröder,
M. Schumacher, K. Wilke

Report No. 101
March 1993
Interannual Variability of Central European Mean Temperature in January / February and its Relation to the Large-Scale Circulation
Peter C. Werner, Hans von Storch
* Climate Research, 1994 in press

Report No. 102
April 1993
Tropospheric Ozone Lidar Intercomparison Experiment, TROLIX '91, Field Phase Report
Jens Bösenberg, Gerard Ancellet, Arnoud Apituley, Hans Bergwerff, Götz v. Cossart, Hans Edner, Jens Fiedler, Bo Galle, Cora de Jonge, Johan Mellqvist, Valentin Mitev, Thorsten Schaberl, Gerd Sonnemann, Jan Spakman, Daan Swart, Eva Wallinder

Report No. 103
April 1993
Modes of Ocean Variability in the Tropical Pacific as Derived from Geosat Altimetry
Jiansheng Zou, Mojib Latif
* Journal of Geophysical Research, in press

Report No. 104
April 1993
Climate Variability in a Coupled GCM
Part II: The Indian Ocean and Monsoon
Mojib Latif, Andreas Sterl, Michel Assenbaum, Martina M. Junge, Ernst Maier-Reimer
* Journal of Climate, in press

Report No. 105
May 1993
Economic Efficiency of CO_2 Reduction Programs
Olli Tahvonen, Hans von Storch, Jinsong von Storch
* Climate Research, 1994, in press

Report No. 106
May 1993
Numerical Experiments on the Atmospheric Response to Cold Equatorial Pacific Conditions ("La Niña") During Northern Summer
Hans von Storch, Dierk Schriever, Klaus Arpe, Grant W. Branstator,
Roberto Legnani, Uwe Ulbrich
* Atmosphere Ocean System 1, 1994, in press

Report No. 107
May 1993
Northern Hemisphere Tropospheric Mid-Latitude Circulation After Violent Volcanic Eruptions
Hans-F. Graf, Judith Perlwitz, Ingo Kirchner
* Contributions to Atmospheric Physics, in press

Report No. 108
July 1993
Decadal Variability of the North Atlantic in an Ocean General Circulation Model
Ralf Weisse, Uwe Mikolajewicz, Ernst Maier-Reimer

Report No. 109
August 1993
Stochastic characterization of regional circulation patterns for climate model diagnosis and estimation of local precipitation
Eduardo Zorita, James P. Hughes, Dennis P. Lettemaier, Hans von Storch

Report No. 110
August 1993
Water tracers in the General Circulation Model ECHAM
Georg Hoffmann, Martin Heimann

Report No. 111
September 1993
Flux aggregation at large scales:
On the limits of validity of the concept of blending height
Martin Claussen

MPI-Report-Reference: *Reprinted in

Report No. 112
September 1993
Reconstruction of the El Niño Attractor with Neural Networks
Björn Grieger, Mojib Latif
* Climate Dynamics, in press

Report No. 113
September 1993
Review Paper **Principal Oscillation Patterns**
Hans von Storch, Gerd Bürger, Reiner Schnur, Jin-Song von Storch
* Journal of Climate, 1994 (in review)

Report No. 114
September 1993
Climatology and Variability in the ECHO Coupled GCM
Mojib Latif, Timothy Stockdale, Jörg-Olaf Wolff,
Gerrit Burgers, Ernst Maier-Reimer, Martina M. Junge
Klaus Arpe, Lennart Bengtsson
* Tellus, in press

Report No. 115
October 1993
Shift of biome patterns due to simulated climate variability and climate change
Martin Claussen

Report No. 116
October 1993
Changing Statistics of Storms in the North Atlantic ?
Hans von Storch, Johannes Guddal, Knut A. Iden, Trausti Jónsson, Jan Perlwitz,
Magnar Reistad, John de Ronde, Heiner Schmidt, Eduardo Zorita

Report No. 117
November 1993
Cloud-turbulence interactions: Sensitivity of a general circulation model to closure assumptions
Sabine Brinkop, Erich Roeckner

Report No. 118
November 1993
Towards a Contrail Climatology from NOAA-Satellite Images over Europe
Stephan Bakan, Margarita Betancor, Veronika Gayler, Hartmut Graßl

Report No. 119
December 1993
Remote sensing of refractivity from space for global observations of atmospheric parameters
Michael E. Gorbunov, Sergey V. Sokolovskiy

Report No. 120
December 1993
Taking Serial Correlation into Account in Tests of the Mean
Francis W. Zwiers, Hans von Storch
*Journal of Climate, 1994 (in press)

Report No. 121
December 1993
Volcanos and El Niño-Signal Separation in Winter
Ingo Kirchner, Hans-F. Graf

Report No. 122
January 1994
Inconsistencies at the Interface of Climate Impact Studies and Global Climate Research
Hans von Storch
* Proc. 13th International Congress of Biometeorology, Calgary, Canada, 1993

Report No. 123
January 1994
Hurricane-type vortices in a general circulation model, Part I
Lennart Bengtsson, Michael Botzet, Monika Esch

Report No.124
January 1994
A Climate Change Simulation Starting at an Early Time of Industrialization
Ulrich Cubasch, Gabi Hegerl, Arno Hellbach, Heinke Höck,
Uwe Mikolajewicz, Benjamin D. Santer, Reinhard Voss

Report No. 125
January 1994
Interdecadal variability in a global coupled model
Jin-Song von Storch
* Tellus, 1994 (in press)

MPI-Report-Reference: * Reprinted in

Report No. 126
February 1994
The influence of cirrus cloud-radiative forcing on climate and climate sensitivity in a general circulation model
Ulrike Lohmann, Erich Roeckner

Report No. 127
January 1994
Sensitivity study of land biosphere CO_2 exchange through an atmospheric tracer transport model using satellite-derived vegetation index data
Wolfgang Knorr, Martin Heimann

Report No. 128
February 1994
Some Sensitivities of a Coupled Ocean-Atmosphere GCM
Timothy Stockdale, Mojib Latif, Gerrit Burgers, Jörg-Olaf Wolff
* Tellus, in press

Report No. 129
March 1994
El Niño/Southern Oscillation
Mojib Latif, J. David Neelin
* Europhysics News

Report No.130
March 1994
' Mixed Boundary Conditions ' in OGCMs and their influence on the Stability of the Model's Conveyor Belt
Uwe Mikolajewicz, Ernst Maier-Reimer

Report No. 131
April 1994
On coupling global biome models with climate models
Martin Claussen

Report No. 132
May 1994
Climate Simulations with the Global Coupled Atmosphere-Ocean Model ECHAM2/OPYC
Part I: Present-day climate and ENSO events
F. Lunkeit, R. Sausen, J. M. Oberhuber

Report No. 133
May 1994
The impact of El Niño-and volcanic forcing on the atmospheric energy cycle and the zonal mean atmospheric circulation
Uwe Ulbrich, Hans-F. Graf, Ingo Kirchner

Report No. 134
June 1994
On the statistical connection between tropospheric and stratospheric circulation of the northern hemisphere in winter
Judith Perlwitz, Hans-F. Graf

Report No. 135
June 1994
A Global Data Set of Land-Surface Parameters
Martin Claussen, Ulrike Lohmann, Erich Roeckner, Uwe Schulzweida

Report No. 136
June 1994
The relationship between sea surface temperature anomalies and atmospheric circulation in general circulation model experiments
Viacheslav V. Kharin

Report No. 137
June 1994
The Social Construct of Climate and Climate Change
Nico Stehr, Hans von Storch

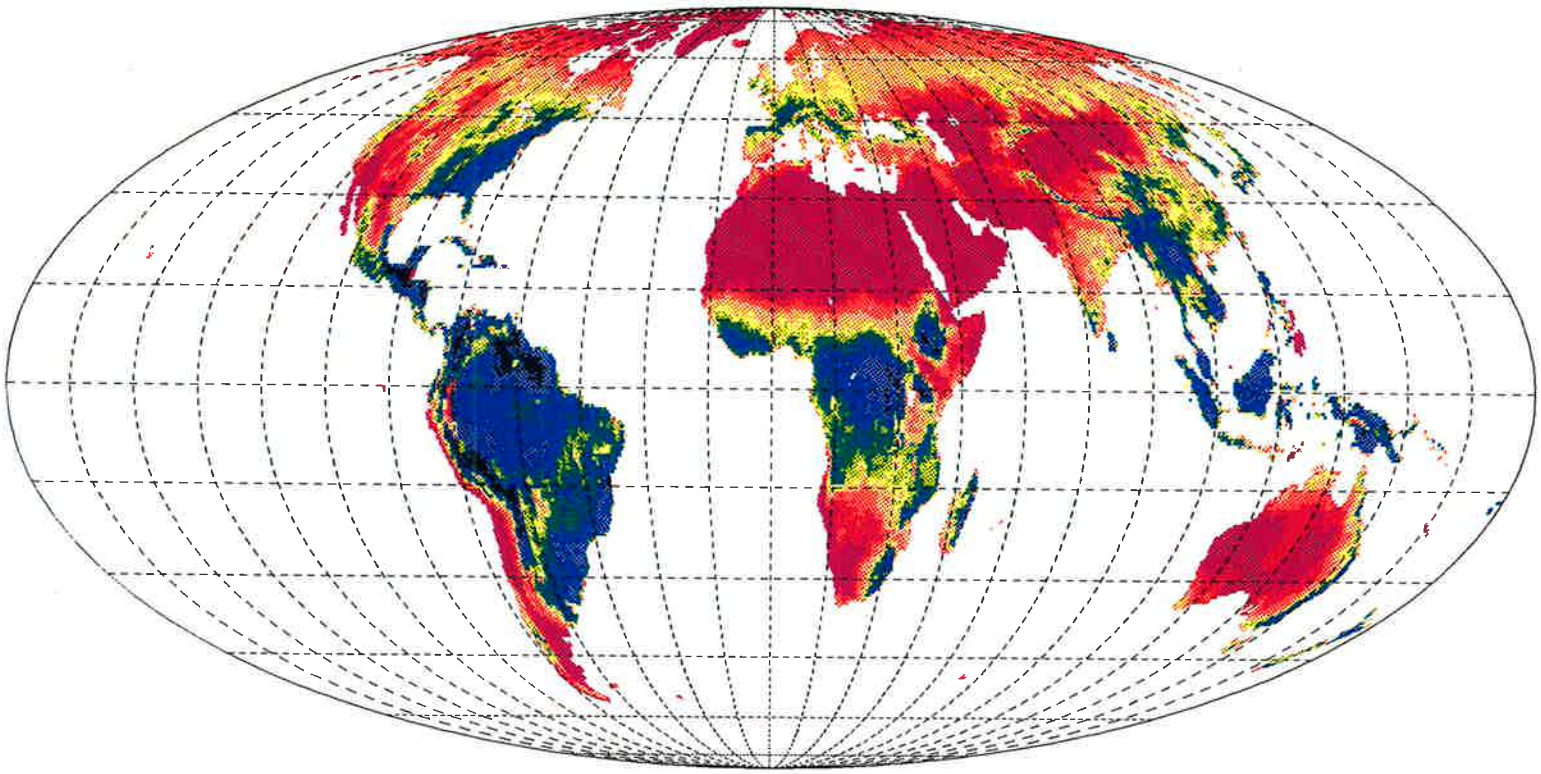

Figure A1: The annual sum of net primary productivity in gC / m^2 according to Formulation I, in equal-area projection. The global sum is 63.1 GtC with A=0.55gC/m^2.

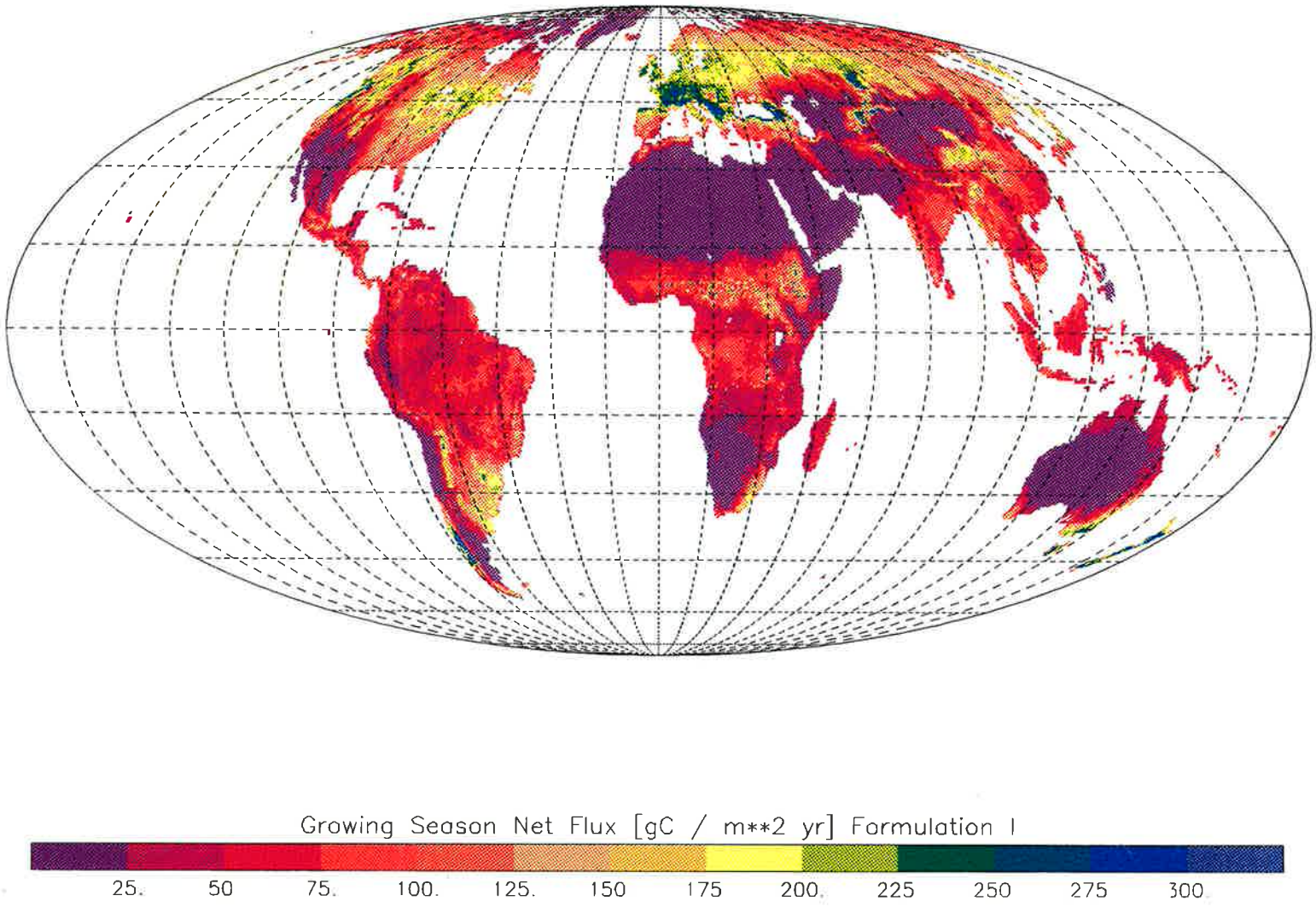

Figure A2: Growing season net flux (GSNF) in gC / m^2 according to Formulation I, with Q_{10}=1.5 and A=0.55gC/m^2. GSNF is defined at each grid point as the sum of the monthly values of NPP minus SR as long as NPP is greater than SR for that month. The global sum of GSNF is 10.2 GtC.